JOURNAL OF MATERIALS SCIENCE 22 (1987) 565–574

The effects of nitrogen additions to a cobalt–chromium surgical implant alloy

Part 1 *Processing and microstructure*

T. KILNER*, A. J. DEMPSEY, R. M. PILLIAR, G. C. WEATHERLY
Department of Metallurgy and Materials Science, University of Toronto, Toronto M5S 1A4, Canada
**Mathematics, Physics and Computer Science Department, Ryerson Polytechnical Institute, 350 Victoria Street, Toronto M5B 2K3, Canada*

The determination of the feasibility of adding nitrogen to a cobalt–chromium implant alloy was undertaken with the ultimate goal of the work being the improvement of the static and fatigue properties of the alloy. Nitrogen additions were made using high-temperature heat treatments in a nitrogen-containing gas atmosphere. The effects of the nitrogen additions were characterized in this study using several techniques. The maximum solid solubility of nitrogen in the alloy at 1200° C (the heat-treatment temperature) was found to be approximately 0.35 wt% N. X-ray diffraction using nitrogen heat-treated powder samples indicated that the addition of nitrogen in solution resulted in a lattice dilation lying in the range of 0.0021 to 0.0035 nm per wt% N. Above the solubility limit, Cr_2N and $Cr_2(CN)$ were present at the nitrogen heat-treatment temperatures in the form of large second-phase particles. Ageing of the alloy containing approximately 0.35 wt% N at 400° C resulted in the precipitation of CrN. A study of the nitrogen distribution suggested that the diffusion of nitrogen was affected by the carbon content of the cobalt-base alloy.

1. Introduction

Porous-surfaced, cobalt alloy orthopaedic implants intended for fixation to bone by osseous tissue ingrowth are currently being used clinically [1]. The porous surface region can be formed by sintering cobalt alloy powder of appropriate size to the surface of a solid cobalt alloy core [2]. To achieve strong particle–particle and particle–substrate bonding, a 1300° C sintering temperature is used for periods of one to three hours [2]. Previous studies have shown that this treatment results in incipient melting of chromium, molybdenum and carbon-enriched interdendritic material, thereby altering the microstructures of the solid core component as well as promoting good particle bonding because of the presence of some liquid phase at the particle boundaries [3]. This sintering method is of obvious benefit to forming these porous-surface structures. However, liquid-phase formation and altered microstructures within the solid core portion of the implant are of concern since good mechanical strength and corrosion resistance are requirements of the final product.

Previous studies in our laboratory have indicated that microstructural changes affect the tensile properties of the alloy [4]. Specifically, it was shown that formation of extensive grain-boundary zones of a $M_{23}C_6$–sigma-phase–cobalt eutectic results in significant reduction in ductility to fracture. Two means of avoiding this unacceptable loss of ductility were proposed, both effectively reducing the carbides present at grain boundaries [5]. First, lowering the carbon content of the core cobalt alloy allows fewer carbides to form. It was shown that by reducing carbon content to approximately 0.10 wt% from its usual value of approximately 0.25 wt%, high elongations to failure resulted despite the 1300° C sintering treatment [5]. Second, by slow cooling from 1300° C to below the eutectic solidification temperature, approximately 1235° C, less grain-boundary eutectic was observed to form, and again, acceptable elongation to fracture resulted [5]. Unfortunately, both methods also result in lower yield strength (i.e. typically 0.2% yield strength equal to 340 MPa after these treatments compared with 450 to 490 MPa for a conventional solution-annealed, 0.25 wt% carbon alloy). Since low yield strengths also are unacceptable for load-bearing implant alloys, a study was undertaken to increase yield strengths using nitrogen as an interstitial solute strengthener in the cobalt alloys. The results of this study are reported in two parts, the first reported herein, dealing with the processing parameters for nitrogen solution strengthening of cobalt-base surgical implant alloys and the second describing the mechanical properties (static and fatigue) of alloys so processed.

A major consideration in varying the composition of any surgical implant alloy is the possibility of altering biocompatibility properties. Increasing nitrogen content was considered suitable in this regard for the following reasons:

0022–2461/87 $03.00 + .12

1. It is commonly present in cast cobalt-based surgical implant alloys (ASTM F75-76) at levels of 50 to 500 p.p.m., and in at least one analysis of a commercially available cobalt implant alloy a value of 2000 p.p.m. was reported [6]. While not included in the ASTM F75-76 specification, its presence seems to be acceptable.

2. Any tendency for obvious detrimental *in vivo* reactions at these composition levels should have become apparent by now. The major known pathological effects of nitrogen in the human body are nitrogen narcosis and Caisson disease (the bends), both of which are the effects of partial pressures of nitrogen well in excess of one atmosphere in the bloodstream.

1.1. Previous studies on nitrogen additions of cobalt alloys

There have been few investigations of the use of nitrogen as a deliberate alloying addition to cobalt alloys. Sieverts and Hagen [7] investigated the Co–N system below the melting point of cobalt and found very low solubility of nitrogen in cobalt. Blossey and Pehlke [8] found that, at 1600° C and 1 atm nitrogen, the solubility of nitrogen in pure liquid cobalt is 0.0047 wt %, while chromium additions (up to 3%) increase the nitrogen solubility and Sievert's law is obeyed. Goldschmidt [9] noted that the only data that he found on ternary systems containing cobalt were for Ti–Co–N, Ta–Co–N and Mo–Co–N. More recent studies on 1 to 3% Ti-bearing cobalt alloys which form titanium nitrides upon nitriding at 982 to 1204° C have been reported. After nitriding, Hartline and Kindlimann [10] found a dispersion of titanium nitrides with a spacing of approximately 10 μm, resulting in a tensile strength of 186 MPa and 1.6% elongation at 1087° C, compared to values for the nitrogen-free alloy of 23 MPa and 11.9% elongation. Rademacher [11] reported a yield strength of 675 MPa and 12% elongation in an F75-76 alloy containing 0.014 to 0.32% carbon and 0.09 to 0.21% nitrogen, with boron additions up to 0.11 wt %. Asgar and Allen [12] claimed that boron additions caused a more uniform distribution of carbides in F75-76 alloys, and a smaller grain size, which could account for the effect observed by Rademacher [11]. Ion nitriding of a cobalt-based hard-facing alloy has also been reported [13]. Recently, Dobbs and Robertson [14] dismissed the use of nitrogen as a solid-solution strengthener in the F75-76 formulation as "of questionable value"; however, no data were presented in support of this statement.

1.2. Commercial nitriding processes

In the absence of any useful information regarding the intentional nitriding of cobalt superalloys, a survey of conventional nitriding processes employed on steels was made [15–18]. The basic reaction during nitriding is the surface diffusion of nitrogen into the component in a nitrogen-containing environment at high temperatures. Correctly done, this leads to high surface hardness, resistance to wear, minimum distortion on heat treatment, resistance to tempering, beneficial effects on fatigue properties, and a marked corrosion resistance in several media.

Nitriding of stainless steel has become increasingly popular recently. This is of particular relevance to the F75-76 alloy as there are important similarities between the two systems. Both alloys have a face-centred cubic crystal structure stabilized by alloying additions and rely on high chromium contents for their corrosion resistance. Nitrogen-strengthened stainless steel is attractive due to its increased strength and abrasion resistance [19].

Kumar *et al.* [20] found that in Fe–18Cr base alloys nitrogen enters the lattice in solid solution in the temperature range 1100 to 1300° C, and that the addition of nitrogen made the alloys fully austenitic, not only at the treatment temperature, but also at room temperature. It has been found that at nitriding temperatures lower than 1137° C, chromium nitrides form in stainless steels, but at temperatures above this the nitrogen remains in solid solution [16]. In addition to the influence of temperature on nitride formation, the concentration of nitrogen in the nitriding gas will also affect nitride precipitate formation. Aghazadeh-Mohandesi and Priestner [21] examined the effect of the nitrogen partial pressure used for gas nitriding on the fatigue endurance limit of a nitrided Fe–18Cr alloy. At high nitrogen partial pressures (> 0.5 atm) the precipitation of Cr_2N was observed at the grain boundaries and within the grains. The maximum increase in endurance limit (10^7 cycles) occurred at the maximum nitrogen content in solution (0.38 wt %). The presence of precipitates at the grain boundaries caused a decrease in the endurance limit to the point where it was comparable to that of the alloy prior to being nitrided. Electron optical investigations have identified chromium nitride and carbonitride precipitates at the grain boundaries as the cause of local chromium depletion and loss of corrosion resistance in stainless steels. It was found that the surface nitrogen content should not exceed 0.35 wt % in stainless steels if a loss of corrosion resistance is to be avoided [22].

To achieve the maximum benefit from the nitriding process it was considered necessary to establish nitriding conditions which would avoid precipitation of nitrides, carbonitrides and/or carbides in the F75-76 alloy. The temperatures used in the nitriding of ordinary steels fall in the range of temperatures at which precipitation of carbides occurs in the cobalt-based alloys (i.e. below 1150° C). This precipitation is accompanied by a loss of ductility [23]. Therefore, it was desirable to heat-treat the cobalt-based alloys at higher temperatures where these carbides are unstable to prevent a loss of ductility.

2. Experimental procedure

2.1. Heat treatment

Heat treatments using nitrogen-containing gases were performed in both a horizontal and vertical SiC element tube furnaces. The specimens for heat treatment were in the form of either tensile bars as specified by ASTM E8-69 (threaded tensile specimens) or thin wafers cut from these tensile bars as described in

Section 2.5. For heat treatments performed in the horizontal furnace, the furnace chamber was flushed with argon initially. The end-cap was then removed and the specimen was loaded against the gas flow into the hot zone. When the vertical tube furnace was used, the specimens were suspended above the hot zone while the furnace was flushed with argon. After several hours of purging, the gas was adjusted to the desired composition for nitrogen heat-treatment and the specimens were lowered into the hot zone. At the end of the heat treatment, the specimens were either water-quenched or allowed to cool in the furnace having been removed from the hot zone. The gases were passed over a dessicant (anhydrous calcium sulphate) and hot zirconium turnings (for oxygen removal) prior to entering the hot zone of the furnace. Ammonia, forming gas (85% nitrogen, 15% hydrogen) and a mixed gas (forming gas and argon) were used in different experimental trials. Heat-treatment temperatures were controlled to $\pm 5°$ C.

2.2. Determination of average nitrogen concentrations

Initial experiments were carried out to determine the average nitrogen content increase associated with different heat-treatment conditions. The 6.25 mm diameter tensile samples used all met the chemical requirements for the ASTM F75-76 specification and had four different initial nominal carbon contents: 0.33, 0.21, 0.19 and 0.14 wt % C. The samples were heat-treated in bundles of four containing one sample of each carbon content. The heat treatments used were as listed below.

2.2.1. Simulated porous coating heat treatment (PC)

This heat treatment simulates the heat treatment required to sinter a porous coating of metallic beads on to a solid substrate, followed by a slow cooling step to minimize the formation of the grain-boundary eutectic phase: 1295° C for 3 h in a vacuum better than 10^{-5} torr, cooled at 1° C min^{-1} to 1200° C, held at 1200° C for 30 min followed by a helium quench [5].

2.2.2. PC and heat treatment in ammonia (PC + AMM)

Following the PC heat treatment the specimens were exposed to ammonia gas for 2 h at 1220° C, followed by 1 h in argon at 1220° C and then quenched into water.

2.2.3. PC and high-temperature heat treatment in ammonia (PC + HT − AMM)

The specimens were subjected to the PC heat treatment and then heat-treated in ammonia at 1300° C for 2 h, cooled at a rate of 1° C min^{-1} to 1220° C, held at 1220° C for 1 h in argon and then quenched into water.

2.2.4. PC and extended solution anneal (PC + ESA)

After the PC heat treatment the specimens were given a solution anneal at 1195° C for 48 h in argon and then quenched into water.

2.2.5. PC and 48 h heat treatment in ammonia (PC + 48AMM)

The PC heat treatment was followed by a 48 h heat treatment at 1195° C in an ammonia atmosphere and then water-quenched.

2.2.6. PC and 48 h heat treatment in forming gas (PC + 48FG)

After the PC heat treatment the specimens were heat treated for 48 h at 1185° C in forming gas and then quenched into water. Transverse slices of reduced sections of the specimens were analysed for nitrogen using a Leco inert gas fusion nitrogen analyser (Leco Corp., St. Joseph, Michigan, USA).

2.3. Nitrogen distribution

As-cast cobalt alloy bars, 12.7 mm diameter by 127 mm long, were trued by machining on a lathe and were then subjected to the PC heat treatment described previously. Low (approximately 0.07 wt %) and high (approximately 0.22 wt %) carbon content bars were heat-treated at 1200° C for periods of 4.5, 12 and 24 h in a mixed gas atmosphere (forming gas and argon) in which the nitrogen content was approximately 25%. In addition, a high-carbon bar was heat-treated in forming gas alone for 24 h. Following each heat treatment the bars were quenched into cold water. Serial sectioning of the heat-treated bars was performed on a lathe. A nitrogen concentration profile was generated by collecting the turnings from each 0.127 mm deep cut and then analysing them for nitrogen using a Leco inert gas fusion nitrogen analyser. This information was used to estimate nitrogen diffusion coefficients in the low and high carbon containing alloys.

2.4. Lattice dilation measurement

A rapidly solidified Co–Cr–Mo alloy powder of similar composition to the cast material was heat-treated for 24 h at 1200° C in a mixture of argon and forming gas selected to create a 25% nitrogen atmosphere. The lattice parameter of this powder, as well as that of the as-received powder which had not been heat-treated in a nitrogen-containing gas, were measured using X-ray diffraction. The powder was sieved to −130 mesh after heat treatment and then loaded into a 0.2 mm capillary along with silicon powder (NBS standard) which acted as an internal standard. A Debye–Scherrer type camera was used with unfiltered copper radiation. Exposure times of 50 to 72 h were used. The resulting very dark film then had one layer of the emulsion removed to allow the characteristic line positions to be measured (resolution = 0.005 mm). Bragg's law was used to convert the angular measurements to values for the apparent lattice parameter. The Nelson–Riley–Sinclair function extrapolation [24] was used to determine the true lattice parameters. Nitrogen content analysis of the nitrogen-treated and as-received powder was performed using the method described previously.

2.5. Transmission electron microscopy of nitrogen-treated specimens

PC + ESA specimens were sectioned through the

TABLE I Carbon and nitrogen analysis of heat-treated cobalt-based alloy specimens. To convert from wt p.p.m. to at p.p.m. multiply by 4.8 for carbon and 4.12 for nitrogen

Alloy (nominal wt % C)	Heat treatment	wt p.p.m. C	wt p.p.m. N
0.33	PC	3313	73
	PC + AMM	2708	364
	PC + HT − AMM	2813	437
	PC + ESA*	2646	73
	PC + 48AMM*	1563	1541
	PC + 48FG*	2188	2791
0.21	PC	2167	243
	PC + AMM	2313	1092
	PC + HT − AMM	2125	777
	PC + ESA*	1563	461
	PC + 48AMM*	1781	1614
	PC + 48FG*	1792	3447
0.19	PC	1896	534
	PC + AMM	1812	558
	PC + HT − AMM	2021	704
	PC + ESA*	1813	206
	PC + 48AMM*	2042	2172
	PC + 48FG*	1583	3544
0.14	PC	1417	437
	PC + AMM	1521	752
	PC + HT − AMM	1125	485
	PC + ESA*	1021	231
	PC + 48AMM*	1583	1954
	PC + 48FG*	1500	3568

*Represents the average of two trials.

threaded region of the tensile samples into wafers approximately 2 mm thick. The wafers were reduced in thickness to 0.2 mm by using an alternating sequence of rolling and annealing. A hardened steel punch was then used to produce 3 mm diameter discs from the 0.2 mm thick sheet.

The resulting discs were heat-treated for 24 h at 1200° C in one of three atmospheres: argon, forming gas, or a mixture of argon and forming gas (25% nitrogen). After heat treatment the foils were either quenched in water or furnace-cooled. The discs were electrolytically thinned for electron microscopic examination using a solution of 5% perchloric acid, 5% glycerol, 55% methanol and 35% butanol with a current of 80 mA and voltage of 45 V at −32° C. The resulting foils had a grain size of about 10 to 20 μm and showed no signs of perforations due to pre-existing porosity.

3. Results

3.1. Average nitrogen content

The results are summarized in Table I. Values of nitrogen reported here represent the average nitrogen content across the entire cross-section of the tensile specimen. It is apparent that in the PC + AMM and PC + HT − AMM specimens the presence or absence of the liquid phase had little or no effect on the average nitrogen contents of these specimens. Both the PC + AMM and the PC + AMM − HT specimens showed increases in the nitrogen content. However, after approximately three hours in ammonia, the maximum increase in nitrogen content was only about 485 wt p.p.m.

The 0.14 wt % carbon specimens which received the PC + ESA heat treatment showed a decrease in nitrogen content when compared to the specimens which underwent only the PC heat treatment. The decrease could be due to fluctuations inherent in the starting material. On the other hand, the 48 h ammonia-treated samples (PC + 48AMM) showed a significant increase in nitrogen content compared with the control samples (PC). The samples treated in forming gas (PC + 48FG) also had greatly increased nitrogen contents.

3.2. Nitrogen distribution

Fig. 1 is a nitrogen concentration profile for a test

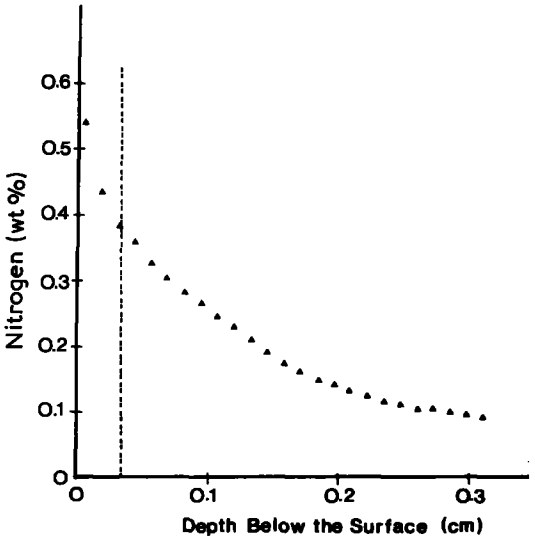

Figure 1 Nitrogen concentration profile for a specimen heat-treated in an 85% nitrogen atmosphere. The vertical dotted line represent the depth to which grain-boundary precipitation was observed.

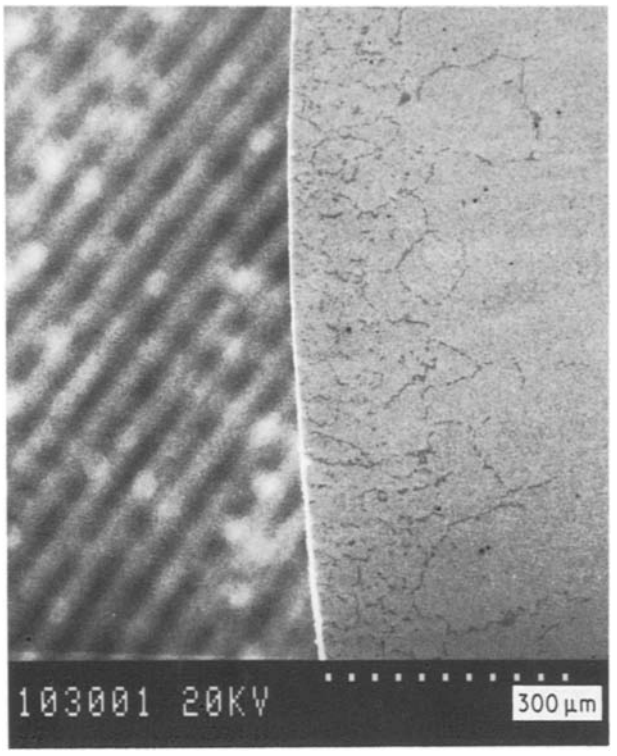

Figure 2 Sample treated in 85% nitrogen atmosphere for 24 h showing chromium nitrides and carbonitrides along grain boundaries at the surface.

specimen heat-treated in forming gas for 24 h. The vertical line represents the approximate limit, from the free surface, of grain boundary precipitation as determined from Fig. 2. Similar precipitation was observed in all the tensile samples heat-treated in forming gas. The appearance of a precipitate suggests that some nitrogen is no longer diffusing as an interstitial solute. Because precipitation affects the diffusion process these samples were not used for estimating diffusion coefficients. Fig. 3 shows the nitrogen concentration profiles for both low- and high-carbon content alloys after being heat-treated for 24 h in an approximately

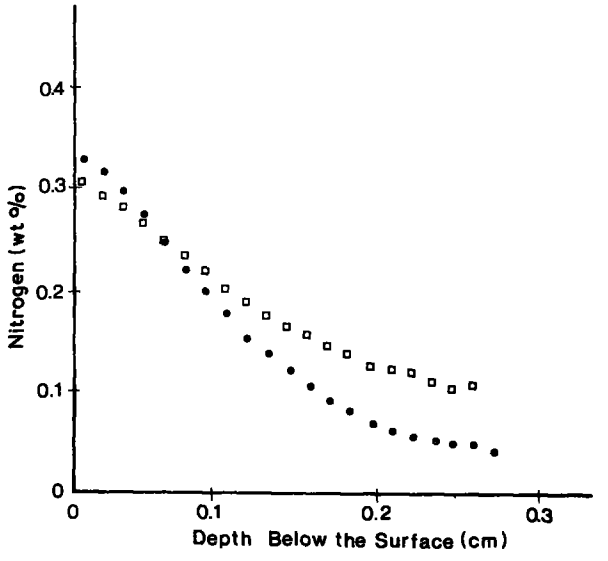

Figure 3 Nitrogen concentration profile for (●) low and (□) high carbon content alloys treated in a 25% nitrogen atmosphere for 24 h.

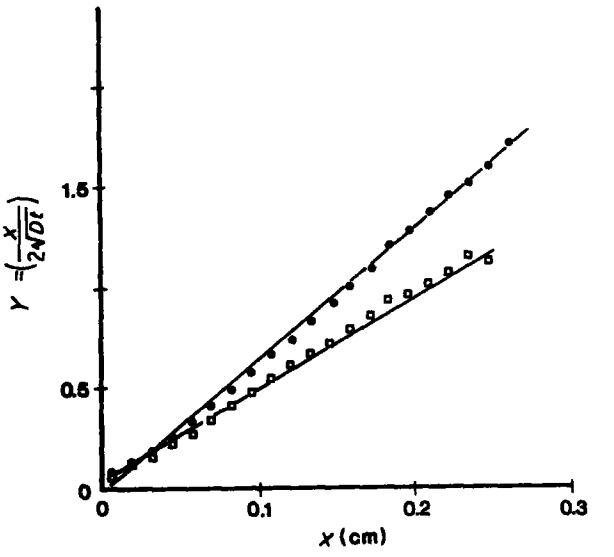

Figure 4 Plot used to calculate nitrogen diffusion coefficients in (●) low and (□) high carbon content cobalt-base alloys. $Y = x/2(Dt)^{0.5}$.

25% nitrogen atmosphere. Similar profiles were generated for heat-treatment times of 4.5 and 12 h. No grain-boundary precipitation, such as that which was observed in the samples treated in forming gas, was detected in these specimens.

Analysis of the diffusivity was carried out using the normalized error function solution to Fick's second law of diffusion:

$$\frac{C_x - C_i}{C_s - C_i} = 1 - \text{erf}(Y) \qquad Y = \frac{x}{2(Dt)^{0.5}} \qquad (1)$$

where C_x = concentration of solute at position x, C_s = concentration of solute at the surface, C_i = concentration of solute at time $t = 0$, erf(Y) = error function, D = diffusion coefficient and t = time. The initial concentration, C_i, was determined by analysing sample turnings from both alloys prior to heat treatment in a nitrogen-containing atmosphere. The surface concentration, C_s, was determined by assuming that the nitrogen content of a small piece of the alloy heat-treated along with the TEM foils (approximately 3900 wt p.p.m.) approximated the equilibrium nitrogen content for the heat-treatment conditions used.

The error-function solution for diffusivity assumes the diffusion is independent of concentration and hence position. Therefore, a plot of Y ($= x/2(Dt)^{0.5}$) against position is linear. The diffusion coefficient was calculated for each concentration (position) data point and the values of D were plotted as Y against position (Fig. 4). The diffusion coefficient was calculated using the equation

$$D = 0.25/(\text{slope}^2 t) \qquad (2)$$

On the basis of these results it appears that the carbon content may influence the diffusivity of nitrogen although the limited data obtained in this study prevent a definite conclusion being reached. The diffusion coefficient for the high carbon content alloy is $7 \times 10^{-8}\,\text{cm}^2\,\text{sec}^{-1}$ and for the low carbon content alloy it is $14 \times 10^{-8}\,\text{cm}^2\,\text{sec}^{-1}$.

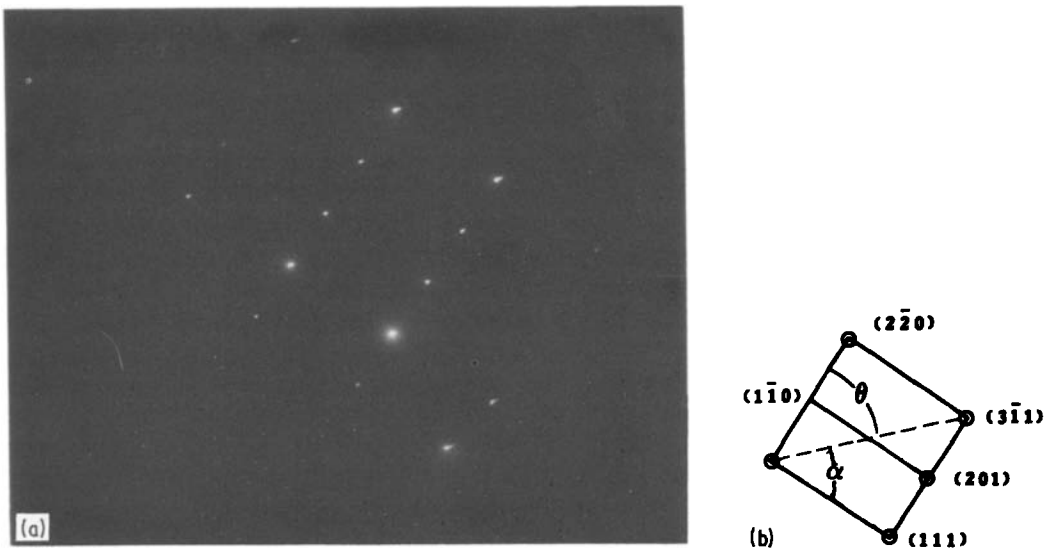

Figure 5 Selected-area diffraction pattern of β-Cr_2N. Identified in sample treated in 85% nitrogen atmosphere at 1200° C for 24 h and water-quenched. Calculated angles $\theta = 44° 52'$, $\alpha = 45° 47'$; zone axis [$\bar{1}\,\bar{1}$2].

3.3. Identification of precipitates in nitrogen-treated samples

3.3.1. Energy-dispersive X-ray analysis

All samples which are treated in forming gas for 24 and 48 h had a second phase along the grain boundaries starting at the specimen surface and penetrating to a distance of 350 to 400 μm. Energy-dispersive microanalysis of this phase showed it to be high in chromium, and to contain smaller amounts of cobalt and molybdenum. This phase could be easily distinguished from the previously established $M_{23}C_6$ carbide [25] on the basis of its chromium to cobalt ratio, since the carbide is found to be consistently lower in chromium content and higher in cobalt.

3.3.2. X-ray diffraction

Since energy-dispersive X-ray microanalysis does not detect carbon or nitrogen due to absorption of the characteristic X-ray photons of these elements by the detector window, electrolytic dissolution of the cobalt-rich matrix of the nitrogen-treated samples in dilute HCl and filtering to obtain a residue of second-phase particles was used to obtain samples for X-ray diffraction identification. This allowed the grain-boundary precipitates near the surface of the forming gas-treated samples to be identified (Fig. 2). They were found to be beta-chromium nitride and chromium carbonitride (ASTM powder diffraction file cards [26] 27-127 and 19-325, respectively). $M_{23}C_6$ was the only second phase detected in similar samples prepared from the central core of the specimens after the outer layer had been digested.

3.3.3. Transmission electron microscopy

The discs prepared as in Section 2.5 showed copious precipitation of large second-phase particles, similar to those previously observed in the tensile specimens treated in forming gas. Selected-area electron diffraction patterns from these second-phase particles agreed with the patterns associated with either beta-chromium nitride or chromium carbonitride structures (Fig. 5). A high stacking-fault density in the cobalt-rich matrix was observed in these samples, but this was determined to be due to quenching since samples which were not quenched showed few stacking faults. Samples which were heat-treated in argon also showed many stacking faults if they had been quenched, but few if they had been furnace-cooled.

Samples treated in mixed gas (argon and forming gas) with a partial pressure of approximately 0.25 atm nitrogen at 1200° C showed that very few second-phase particles result from this concentration of nitrogen in the atmosphere of the furnace. Indirect confirmation that nitrogen actually was present in these foils was obtained by including a larger sample of F75-76 with the discs when they were heat-treated. Subsequent chemical analysis of this sample gave a nitrogen content of 3900 wt p.p.m. There were a few second-phase particles approximately 3 μm in diameter which gave diffraction patterns which could be identified as beta-chromium nitride or carbonitride. Nothing was observed in the foil samples which would indicate the presence of a precipitate of a size and density necessary to cause appreciable strengthening effects, and no diffraction effects (such as streaking of spots) were noted which would indicate the presence of a very fine precipitate. Again, as in the previous studies, thin foils quenched after heat treatment contained a high density of stacking faults while those cooled more slowly contained none.

As additional proof that nitrogen was present in solution in high concentration in the foils treated in the mixed gas, the nitrogen-rich foils were subsequently maintained at a temperature of 400° C in the electron microscope for periods up to 40 min. During this time, a large number of randomly oriented precipitate particles developed (Fig. 6). These particles appear to have nucleated at the surface of the foils, because the density appeared constant regardless of the foil thickness, and tilting the foil in the microscope produced no contrast effects. The rapidity of precipitation is probably due to the added influence of the high-energy electrons in the beam interacting with the relatively low mass nitrogen atoms, speeding their

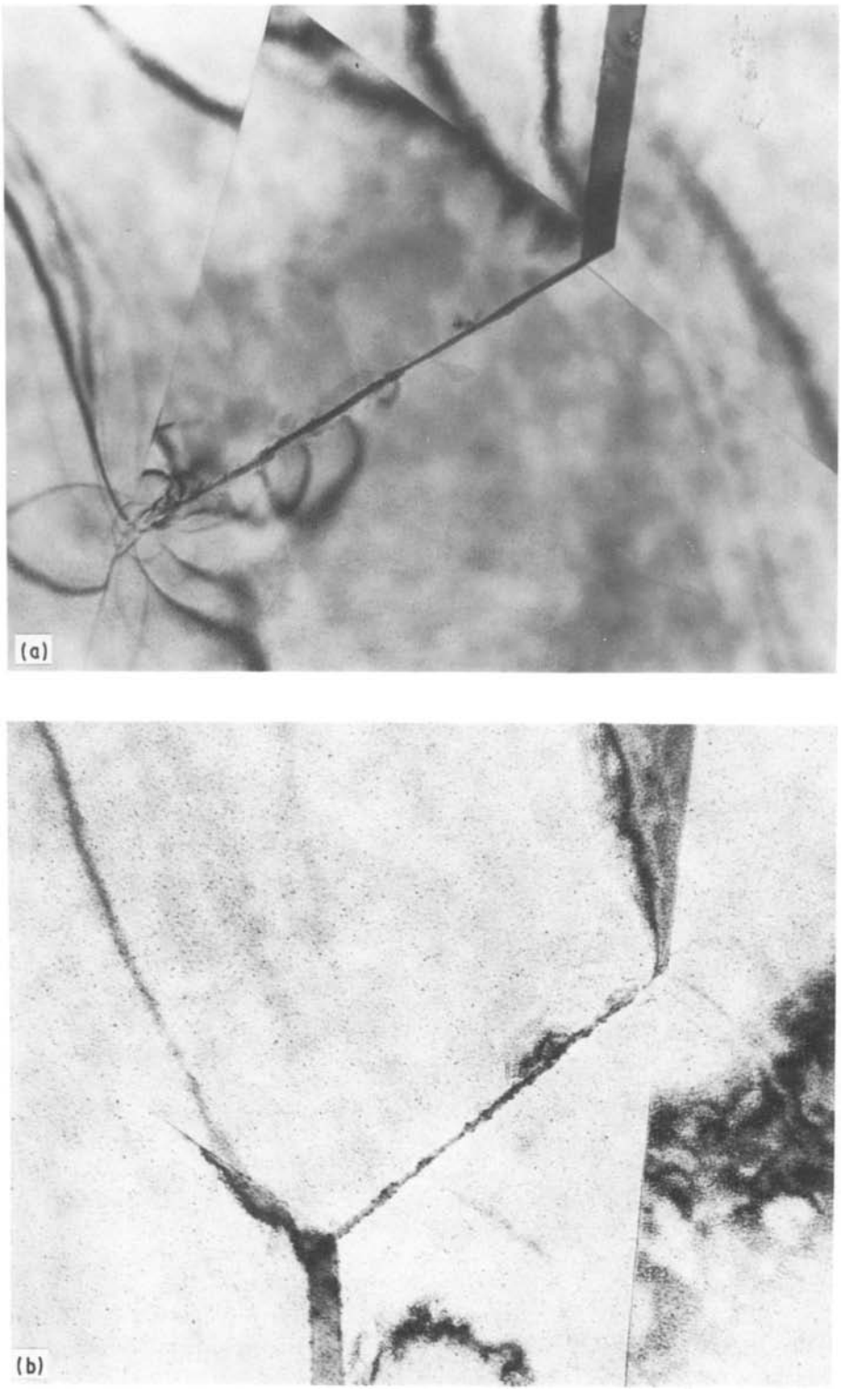

Figure 6 Development of precipitate in aged foils. Sample initially treated in 25% nitrogen atmosphere for 24 h at 1200° C. (a) Appearance prior to ageing (× 14 400); (b) appearance after ageing 40 min at 40° C (× 14 400).

diffusion. The precipitation could also be affected by the environment in the microscope, although this is unlikely as the vacuum was better than 10^{-7} torr.

The precipitate in the foils aged in the microscope was easily identified from the electron diffraction pattern (Fig. 7). Using the cobalt-matrix reflections as a standard, the rings were found to fit CrN exactly. CrN is a cubic, NaCl-type structure with $a = 0.41$ nm (ASTM 11-65) [27].

3.4. Lattice dilation

Fig. 8 is a plot of the N–R–S function against the apparent lattice parameter for the nitrogen-treated powder and for the as-received powder. The change in the lattice parameter corresponds to a lattice dilation coefficient lying in the range of 0.0021 to 0.0035 nm per wt % N. This range represents the maximum and minimum dilation coefficients calculated using the standard error associated with each intercept.

4. Discussion

4.1. Indentification of precipitates

The identification of the second phase suggests that $M_{23}C_6$, β-Cr_2N and Cr_2 (CN) are simultaneously present in the Co–Cr–Mo alloy. This observation is in qualitative agreement with predictions of the Cr–C–N

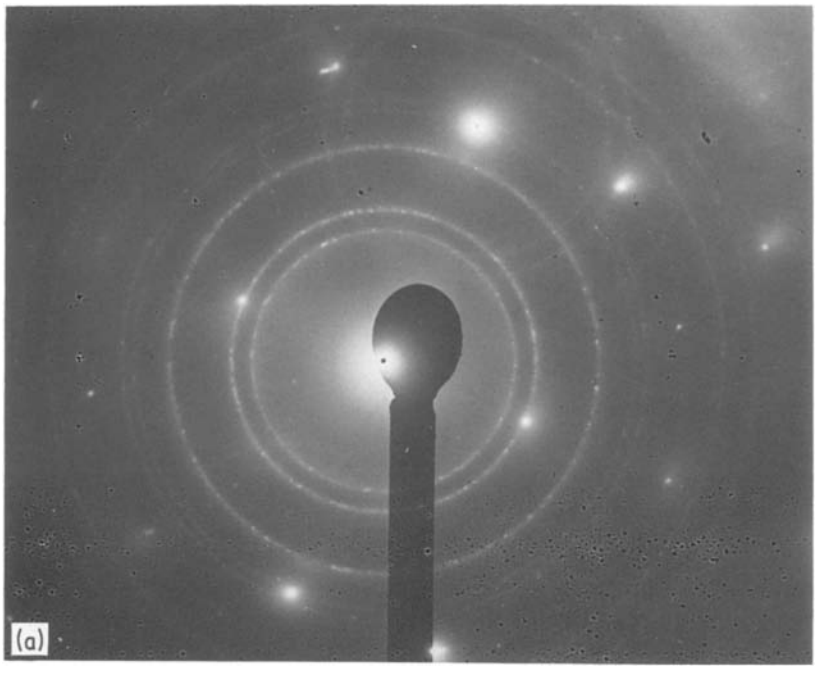

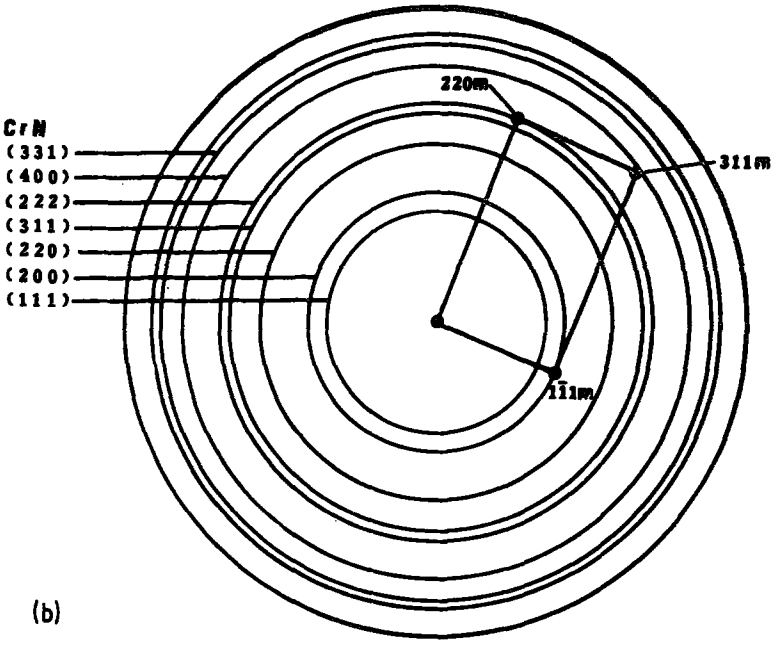

Figure 7 (a, b) Diffraction pattern from precipitate in aged samples (400° C, 40 min). Identified as CrN. m = matrix spots.

phase diagram (Fig. 9). Chromium has a much stronger interaction with the interstitial elements carbon and nitrogen than exists between cobalt and these elements. Because cobalt acts only as an inert matrix within which the precipitation reactions take place, it is reasonable to use the Cr–C–N phase diagram to predict precipitation reactions in the Co–Cr–Mo alloy system.

The precipitated phases identified in the nitrogen-treated cobalt alloy agree with the predictions of the Cr–C–N phase diagram in the range 1100 to 1400° C [27]. While the precipitates undoubtedly contain small amounts of molybdenum and cobalt, in essence, they are chromium nitride or carbonitride. The CrN precipitate formed on ageing at 400° C was not analysed for composition, but probably also contained traces of cobalt and molybdenum. According to Jack [28], in Fe–Cr alloys, CrN is more stable than Cr_2N at temperatures below 575° C, and is precipitated for any chromium content. At 865° C, CrN will precipitate in alloys with less than 14 wt % chromium. Thus, Cr_2N is favoured at high temperatures and high chromium contents. This observation agrees qualitatively with the results of this study on a Co–Cr alloy.

4.2. Diffusion

The diffusion coefficients calculated for this alloy system are similar to those measured for the diffusion of nitrogen in austenitic stainless steels which have been heat-treated under similar conditions (Table II). There are several similarities between the Co–Cr and the Fe–Cr systems which make the ferrous system a useful basis for comparison when considering the diffusion of an interstitial solute (e.g. carbon, nitrogen). Both alloy systems have an f c c structure, with similar lattice parameters (typically 0.357 to 0.360 nm). This suggests that the free volume available for diffusion of an interstitial atom is similar for the two alloys. In addition to possessing common structural features, there are chemical similarities. The major alloy

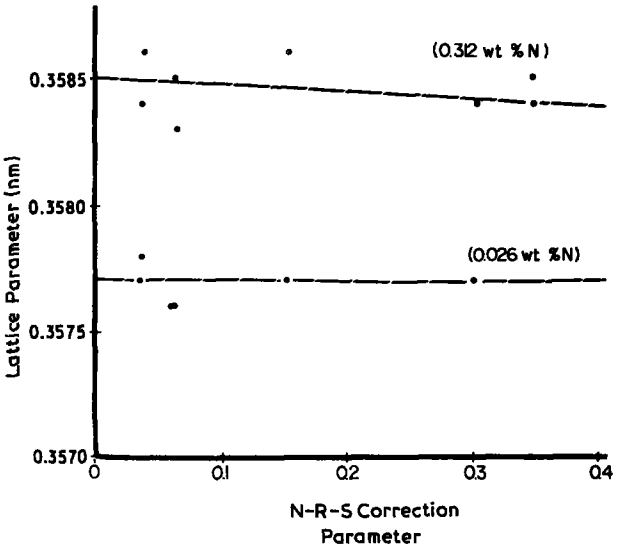

Figure 8 Change in lattice parameter of the cobalt alloy due to increased nitrogen content.

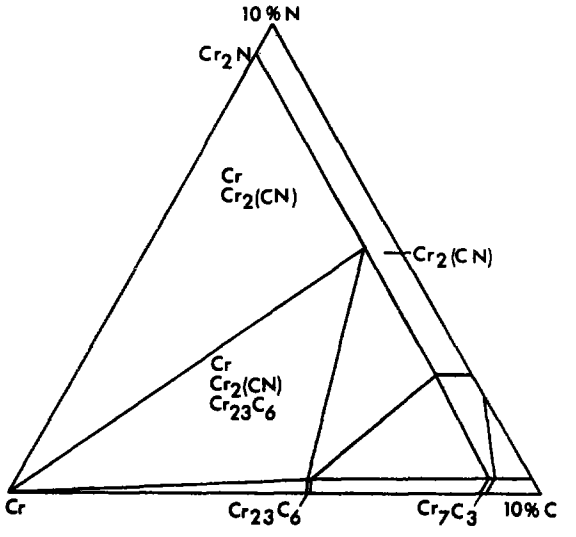

Figure 9 C–Cr–N isotherm at 1100° C. Compositions in wt %.

addition for both alloy systems is chromium, which affects the solubility and the mobility of carbon and nitrogen atoms.

The trend towards a dependence of the diffusion coefficient on carbon content is also supported by observations made in ferrous alloy systems. The diffusion of carbon in austenitic alloys increases with increasing carbon content for two reasons. Firstly, dissolved carbon in this alloy occupies the octahedral interstitial sites, but its atomic size exceeds the size of these sites. The result of the misfit is a dilation of the lattice which makes the diffusion of an interstitial solute easier due to the increased free volume present in the matrix. Secondly, the thermodynamic activity of the carbon increases with increasing concentration of carbon which also leads to more rapid diffusion. It may be that the carbon present in this Co–Cr–Mo alloy has a similar effect on the diffusion of nitrogen.

4.3. Lattice dilation

The observation of a lattice dilation associated with nitrogen heat-treatment of the alloy in a 25% nitrogen atmosphere suggests that the nitrogen is primarily in solution: this is in agreement with the TEM findings. For the addition of nitrogen to pure iron [29] and to chromium–nickel austenitic steels [30] the dilation was reported to be 0.0030 mm (per wt % N). Thus, it appears the experimental range of 0.0021 to 0.0035 nm per wt % N found in this study for the F75-76 alloy is a reasonable estimate.

5. Conclusions

1. Transmission electron microscopy showed that nitrogen was present in solid solution in the cobalt-based alloy heat-treated in nitrogen-containing atmospheres at concentrations up to about 0.35 wt % at 1200° C. Powder X-ray diffraction confirmed that nitrogen enters the lattice in solution resulting in an expansion of the lattice. At higher nitrogen concentrations, chromium nitride and carbonitride precipitates formed during heat treatment at 1200° C.

2. The diffusion coefficient of nitrogen was measured in both the high- and low-carbon content cobalt-base alloy. The diffusion coefficient was larger for the high carbon content alloy (14×10^{-8} compared with $7 \times 10^{-8}\,cm^2\,sec^{-1}$) indicating that carbon content may influence the diffusivity of nitrogen.

3. The precipitates which formed when the cobalt-based alloy was heat-treated in high nitrogen potential atmospheres were identified as beta-chromium nitride and chromium carbonitride. This finding is in qualitative agreement with the predictions of the behaviour expected from the ternary Cr–C–N phase diagram.

4. The addition of nitrogen to the cobalt-base alloy as an intersitial solute is accompanied by a lattice dilation lying in the range of 0.0021 to 0.0035 nm per wt % N.

Acknowledgements

The authors would like to acknowledge the financial support of Canadian Oxygen Limited and the Natural Sciences and Engineering Research Council of Canada.

TABLE II Diffusion coefficients for nitrogen in austentic stainless steels

	Reference	
	[21]	[20]
Material composition (wt %)	0.12 to 0.16C; 0.76 to 1.82Mn; 17.86 to 18.6Cr; < 0.01 to 2.02Mo; 9.22 to 9.75Ni; < 0.01 to < 0.1Ti; balance Fe	0.01 to 0.05C; 17.8 to 18Cr; 0.01 to 14.9Mn; 2.1 to 4.95Ni; balance Fe
Atmosphere	N_2/H_2–25 to 95% N_2	N_2/H_2–20 to 50% N_2
Temperature (° C)	1160	1200
Diffusion coefficient ($cm^2\,sec^{-1}$)	$12.7 \pm 0.04 \times 10^{-7}$	$3.0 \pm 1.0 \times 10^{-7}$

References

1. C. A. ENGH, *Clin. Orthop.* **176** (1983) 52.
2. R. M. PILLIAR, *ibid.* **176** (1983) 42.
3. T. KILNER, G. C. WEATHERLY and R. M. PILLIAR, *Scripta Metall.* **16** (1982) 741.
4. T. KILNER, R. M. PILLIAR and G. C. WEATHERLY in Transactions of 8th Annual Meeting of the Society of Biomaterials, Orlando, April 1982 (Society for Biomaterials) p. 94.
5. T. KILNER, W. M. LAANEMAE, R. M. PILLIAR and G. C. WEATHERLY, *J. Mater. Sci.* **21** (1986) 1349.
6. J. COHEN, R. M. ROSE and J. WULFF, *J. Biomed. Mater. Res.* **12** (1978) 935.
7. J. SIEVERTS and H. HAGEN, *Z. Physik. Chem. A* **169** (1934) 237.
8. G. R. BLOSSEY and R. D. PEHLKE, *Trans. AIME* **236** (1966) 28.
9. H. J. GOLDSCHMIDT, "Interstitial Alloys" (Butterworths, London, 1967) p. 239.
10. A. G. HARTLINE and L. E. KINDLIMANN, *Ger. Offen.* 2614414 (1976).
11. L. RADEMACHER, *Ger. Offen.* 2 225 577 (1973).
12. K. ASGAR and F. C. ALLEN, *J. Dent. Res.* **47** (1968) 189.
13. C. PANZERA and G. A. SALTMAN, *Wear Mater.* **2** (1979) 441.
14. H. S. DOBBS and J. L. M. ROBERTSON, *J. Mater. Sci.* **18** (1983) 391.
15. K. H. JACK, in Proceedings of Symposium on High Temperature Gas–Metal Reactions in Mixed Environments, Boston, May 1972 (Metals Society, AIME, New York, 1972) p. 182.
16. "Source Book on Nitriding" (ASM, Metals Park, 1977) p. 219.
17. "Carburizing and Carbonitriding" (ASM, Metals Park, 1977) p. 125.
18. H. W. McQUAID and W. J. KETCHUM, *Trans. Amer. Soc. Steel Treating* **14** (1928).
19. H. E. CHANDLER and D. F. BAXTER, *Met. Prog.* **125** (1) (1984) 60.
20. D. KUMAR, A. D. KING and A. D. BELL, *Met. Sci.* **17** (1983) 32.
21. J. AGHAZADEH-MOHANDESI and R. PRIESTNER, *Met. Tech.* **10** (1983) 89.
22. T. L. ELLISON, R. H. SHAY and K. R. BERGER, *Met. Prog.* **123** (7) (1983) 37.
23. R. N. J. TAYLOR and R. B. WATERHOUSE, *J. Mater. Sci.* **18** (1983) 3265.
24. C. S. BARRETT and T. B. MASSALSKI, "Structure of Metals", 3rd Edn (McGraw-Hill, New York, 1966) p. 141.
25. T. KILNER, R. M. PILLIAR, G. C. WEATHERLY and C. ALLIBERT, *J. Biomed. Mater. Res.* **16** (1982) 63.
26. "Powder Diffraction File", Joint Committee on Powder Diffraction Standards (American Society for Testing and Materials, Philadelphia).
27. "ASM Metals Handbook", Vol. 8, 8th Edn (ASM, Metals Park, 1972).
28. K. H. JACK, in "Heat Treatment '73", Proceedings of Conference, London, December 1973 (The Metals Society, London, 1975) p. 39.
29. N. RIDLEY, *J. Iron Steel Inst.* **209** (1971) 396.
30. M. KIKUCHI, T. TANAKA, K. HAMAGAMI, Y. OGURA and R. TANAKA, *Met. Trans. A* **7A** (1976) 906.

Received 26 March
and accepted 5 June 1986